Recombination Fluorescence in Ultracold Neutral Plasmas

S. D. Bergeson[1] and F. Robicheaux[2]

[1]Department of Physics and Astronomy, Brigham Young University, Provo, Utah 84602, USA
[2]Department of Physics, Auburn University, Auburn, Alabama 36849, USA

(Received 21 August 2007; revised manuscript received 9 May 2008; published 15 August 2008)

We present the first measurements and simulations of recombination fluorescence from ultracold neutral calcium plasmas. This method probes three-body recombination at times less than 1 μs, shorter than previously published time scales. For the lowest initial electron temperatures, the recombination rate scales with the density as $n_0^{2.2}$, significantly slower than the predicted n_0^3. Recombination fluorescence opens a new diagnostic window in ultracold plasmas. In most cases it probes deeply bound level populations that depend critically on electron energetics. However, a perturbation in the calcium $4snd$ Rydberg series allows our fluorescence measurements to probe the population in weakly bound levels that result just after recombination.

DOI: 10.1103/PhysRevLett.101.073202 PACS numbers: 34.80.Lx, 52.27.Cm, 52.27.Gr

The study of relaxation dynamics in strongly coupled systems is a significant and complicated problem. Strong coupling occurs when the ratio of potential energy per particle to the kinetic energy is greater than unity. This occurs in some astrophysical environments, quark-gluon plasmas, the Bose-Einstein condensation-BCS crossover, the Mott-insulator transition, non-neutral and dusty plasmas, and other systems.

Ultracold neutral plasmas are strongly coupled systems. They are created by photoionizing laser-cooled atoms and can be just inside the strong coupling regime with $\Gamma \equiv (e^2/4\pi\epsilon_0)(4\pi n/3)^{1/3}(k_B T)^{-1} \geq 1$. The plasma electrons have little kinetic energy and are bound to the space charge of the ions. They are in a metastable nonequilibrium state and eventually relax to the ground state. Previous studies have focused on relaxation into high-lying states via three-body recombination (TBR), disorder-induced heating, and plasma expansion [1–19].

In this Letter we present a new relaxation study in ultracold neutral plasmas. We measure and numerically simulate fluorescence emitted by the plasma following electron or ion recombination for a range of initial plasma densities and electron temperatures. This study focuses on TBR during the first microsecond of plasma evolution, which is earlier than any previous work. Fluorescence methods probe deeply bound states, making it possible to measure the evolving electron energy distribution at the earliest times. While we see significant departure from the expected TBR density scaling, we find no compelling departure from the standard TBR model for $t \leq 1$ μs.

Three-body recombination is well understood in weakly coupled plasmas. An electron and ion collide in the presence of another electron. The TBR rate (per atom) is the two-body collision frequency multiplied by the probability that a third body is one collision distance away. The rate scales with density n and temperature T, as $\gamma_{\mathrm{TBR}} = \mathcal{R} n^2 T^{-9/2}$, where $\mathcal{R} = 0.76(e^2/4\pi\epsilon_0)^5 m_e^{-1/2} k_B^{-9/2}$ is the TBR rate coefficient [12,20].

In strongly coupled plasmas, this picture breaks down. The average distance between electrons becomes comparable to the collision distance. The electrons are in constant "collision" and TBR becomes, in a sense, many-body recombination. Numerical and theoretical work predict changes in TBR in strongly coupled plasmas [12,21]. However, there is no experimental evidence for departure from the standard formulas.

The $T^{-9/2}$ dependence makes TBR a sensitive probe of the electron temperature [16], although no measurements exist at times less than 1 μs. The electron system equilibrates on the shortest time scales and largely determines how the plasma expands. The minimum electron temperature, set by disorder-induced heating, is the correlation temperature, $T_c = e^2/4\pi\epsilon_0 a_{\mathrm{WS}} k_B$, where $a_{\mathrm{WS}} = (3/4\pi n)^{1/3}$ is the Wigner-Seitz radius [22]. This temperature is reached on the time scale of the inverse plasma frequency, $1/\omega_p = \sqrt{\epsilon_0 m_e/ne^2}$. Recombination and electron-Rydberg scattering continue to heat the electron system, although on much longer time scales [9,12,13,18].

Our ultracold plasmas are created by photoionizing laser-cooled calcium atoms in a magneto-optical trap [3]. The plasma density profile is approximately Gaussian and spherically symmetric with the density $n(r, t) = n_0 \exp[-r^2/2w^2(t)][w_0/w(t)]^3$, where t is the time after photoionization, $w(t) = \sqrt{w_0^2 + v_{\mathrm{th}}^2 t^2}$, $w_0 = 0.35$ mm, and v_{th} is the rms ion velocity. In thermodynamic equilibrium, this is the rms thermal velocity, $\sqrt{kT/m}$. For a self-similarly expanding ultracold plasma at late times, this tends towards the rms expansion velocity, $\sqrt{kT_e/m_i}$. The initial ion temperature is equal to the neutral atom temperature (~1 mK). The initial electron energy is equal to the difference between the photoionization laser photon

energy and the atomic ionization energy. The lower limit is set by the laser bandwidth to approximately $2E_e/3k_B = 0.5$ K. The two-step photoionization process ionizes nearly 100% of the atoms in the magneto-optical trap (MOT), and our maximum plasma density is set by the MOT density to $n_0 \leq 2 \times 10^{10}$ cm^{-3}.

Fluorescence from the plasma is collected by a fast lens system and detected using a photomultiplier tube. A typical fluorescence curve is shown in Fig. 1. An interference filter blocks light from the photoionizing and MOT laser beams and transmits fluorescence photons at 410 nm. At early times, the fluorescence signal grows as recombination proceeds. After a few μs the plasma expands and the density decreases. The fluorescence signal falls as recombination slows down and the plasma moves out of the view of the fluorescence collection optics.

Normally one would expect the fluorescence signal to be the end product of a series of collision events [23]. Free plasma electrons and recombined Rydberg atoms are in a quasiequilibrium. The near balance between recombination and ionization gives rise to the thermal bottleneck, which is a minimum in the Rydberg state distribution at few $-k_BT$ [12]. A collision occasionally occurs that puts the atom in a Rydberg state below the bottleneck. The number of recombined atoms is proportional to n_0^3. An additional electron collision deexcites these atoms to more deeply bound radiating levels. The additional collision step gives the fluorescence signal an n_0^4 dependence.

In calcium the situation is different. The $4snd$ Rydberg series is strongly perturbed [24]. Rydberg levels that should be long-lived are mixed with the $3d^2$ or $3d5s$ states [25] which add oscillator strength for fast radiative transitions to deeply bound energy levels. This essentially bypasses the collisional deexcitation step and changes the density dependence of the fluorescence signal.

We numerically simulate recombination and fluorescence in the plasma using a method similar to

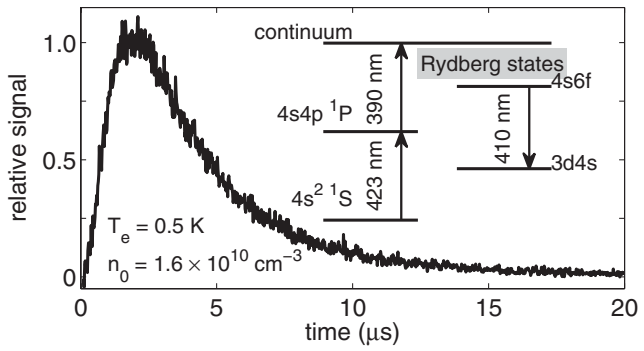

FIG. 1. Recombination fluorescence signal at 410 nm. The time at which the fluorescence signal peaks depends on the density, with higher density plasma signals peaking earlier than low density plasmas. At 1 μs, the plasma density has changed by 10% due to expansion. Inset: Partial energy level diagram for neutral calcium.

Refs. [13,14]. We assume the plasma to be nearly charge neutral with a spherically symmetric Gaussian density distribution. The electrons are in thermal equilibrium at a temperature T and the plasma expands self-similarly. The equations of motion at this level of approximation are described in Sec. IIIc of Ref. [14]. The plasma expansion decreases the thermal energy of the electrons while increasing the radial speed of the ions. When recombination occurs, the density decreases and the temperature increases. An electron collision with an atom that decreases the atom's energy increases the electron temperature and vice versa.

We compute the evolving atom population using a Monte Carlo technique. During a time step, we compute the probability of formation of an atom into a particular state at each position r using the method of Sec. IV of Ref. [14]. This gives more atoms formed at the center of the plasma where the density is high, and the atoms are predominantly in high Rydberg states [26,27]. The radial velocity of the atom is taken to be the radial velocity of an ion at the position the atom is formed. After the atom is formed, we track its position and velocity so we know the correct electron density near each atom and we know whether the atom is within the detection region when the photon is emitted. After the atom is formed, its state changes due to electron collisions and radiative decay. The electron collisions can reionize the atom, excite it to higher energies, or deexcite it. The electron collision processes are computed with a Monte Carlo technique using the rates of Ref. [20]. One difference with Ref. [14] is that we used the exact hydrogenic radiative decay rates for $n\ell \rightarrow n'\ell'$ for $n \leq 30$. We did this because the ℓ states are not necessarily statistically mixed for lower n and the fluorescence signal depends on correctly computing the cascade. When an atom's principle quantum number drops below 5 it is counted as a fluorescence photon and removed from the simulation.

We approximate the $3d^2$ and $3d5s$ state mixing into the Rydberg levels by placing a perturbing level 150 cm^{-1} below the ionization limit with a width of 150 cm^{-1} [25]. The radiative decay rates of the perturbing level is a parameter in the simulation. For physically reasonable estimates, the time dependence and density scaling of the fluorescence signal are largely independent of the exact rate at early times in the plasma evolution.

The simulation and experiment are compared in Fig. 2. At higher initial electron temperatures the fluorescence signal scales as n_0^3. This clearly shows the influence of the perturbing levels in the radiative cascade process. These results suggest that the calcium fluorescence signal is proportional to the Rydberg atom density. This surprising result suggests that a rate equation model treating all Rydberg states equally and neglecting transitions between Rydberg levels can be used to interpret the fluorescence signal.

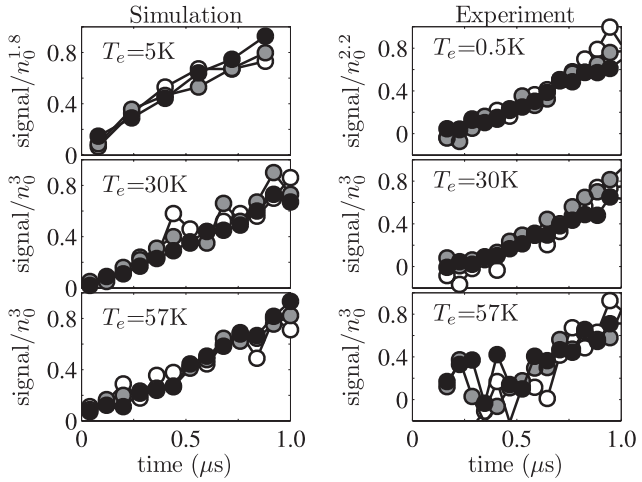

FIG. 2. A comparison of the simulation and experiment. For $T = 30$ and 57 K, the simulated and experimental fluorescence signals both scale with n_0^3 [see Eq. (3)]. The simulation plots are for densities of 5, 10, and 20×10^9 cm^{-3}, corresponding to nonequilibrium initial values of $\Gamma = 0.08$, 0.10, and 0.13 for $T = 57$ K and $\Gamma = 0.15$, 0.19, and 0.24 for $T = 30$ K. The densities in the experimental plots cover the same range. White, gray, and black circles plot the low, medium, and high densities. For this figure, the fluorescence signal is divided by density raised to the indicated power, and each set of plots is scaled for comparison. The 100–200 ns delayed onset of the experimental signal probably indicates the time required for the electrons to fill out a Boltzmann distribution.

The rate at which Rydberg atoms are formed in the plasma can be written as

$$\frac{dn_r}{dt} = -\mathcal{S} n_r n_e + \mathcal{R} n_e^3 T^{-9/2}, \tag{1}$$

where $\mathcal{S}$ is the collisional ionization rate and $n_r(n_e)$ is the Rydberg atom (electron) density. At early enough times, we can neglect the collisional ionization term because n_r is small. The plasma is approximately charge neutral ($n_e + n_r = n_0$), and the solution to Eq. (1) is

$$n_r(t) = n_0[1 - (1 + 2n_0 \mathcal{R} T_e^{-9/2} t)^{-1/2}] \tag{2}$$

$$\approx n_0^3 \mathcal{R} T_e^{-9/2} t, \tag{3}$$

where the approximation results from a binomial expansion assuming that the recombined fraction is small ($n_0^2 \mathcal{R} T_e^{-9/2} t \ll 1$). We can use the analytic expression for $\mathcal{R}$ to write Eq. (3) as

$$n_r(t) \approx 0.1 n_0 \omega_p \Gamma^{9/2} t, \tag{4}$$

similar to an expression derived in Ref. [12]. When Γ is a constant the recombination signal scales with density as $n_0^{3/2}$. For plasmas with the lowest initial electron temperatures, this condition is met at two different times in the plasma evolution. The first is at the earliest times, after one plasma period and before significant recombination has occurred, when $\Gamma = 1$. The second time is late in the plasma evolution, when the balance between adiabatic expansion, recombination, and electron-Rydberg scattering has clamped Γ to be approximately 0.2 [9,13,15]. Approximations used in the foregoing analysis prevent strict quantitative predictions when $\Gamma \geq 1$. However, the simulation provides qualitative estimates for recombination as the strongly coupled regime is approached.

We measure the recombination fluorescence signal for plasmas with an initial electron temperature of 57, 30, and 0.5 K over a range of densities. As predicted by this model and reproduced in our simulations, the slope of the initial fluorescence signal is linear in time (Fig. 2). For $T = 57$ and 30 K, the slope scales as n_0^3 as shown in Fig. 3 and in agreement with Eq. (3).

For the densities in Fig. 3, the correlation temperature ranges from $T_c = 4$ to 7 K [22]. The 57 and 30 K measurements are made with $T \gg T_c$. Equation (3) indicates that the ratio of the slopes at these two temperatures should be $(57/30)^{9/2} = 18$. Instead, we see a factor of 5, suggesting that the actual electron temperature is not 30 K, but rather $57/5^{2/9} = 40$ K. This is comparable to the temperature predicted by our simulation. It has increased from 30 K due to recombination and electron-Rydberg scattering.

For $T = 0.5$ K, the initial fluorescence slope changes as $n_0^{2.2}$. After one plasma period (<1 ns), disorder-induced heating quickly raises the electron temperature from 0.5 to about 5 K ($T \sim T_c$, depending on density) and $\Gamma = 1$. Thereafter, the temperature increases more slowly, around $1.5 \times 10^{-3} T_c$ per plasma period [12]. The Γ changes from 1 at $t = 1/\omega_p$ to 0.5 or 0.2 at 500 ns, depending on the initial density. Although the recombined fraction is approximately 0.1 at 500 ns, Γ evolves during our measurement time.

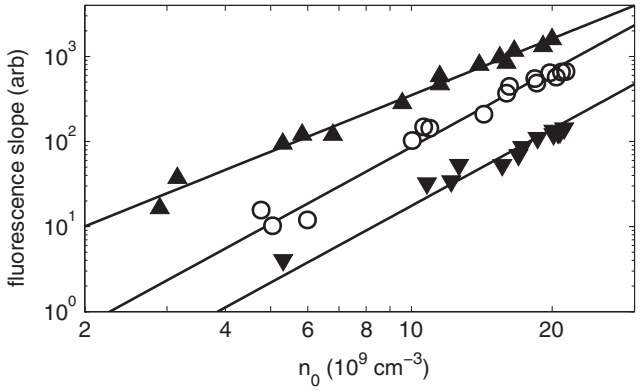

FIG. 3. The slope of the initial recombination fluorescence signal as a function of initial electron temperature and density. $T_e = 57$ K (black upside-down triangles), $T_e = 30$ K (circles), and $T_e = 0.5$ K (black triangles). The higher temperature signals scale as n_0^3, in agreement with Eq. (3). The lowest temperature scales as $n_0^{2.2}$, contrary to Eq. (4).

Depending on the density, our simulations give a temperature increase to 15 K at low density up to 50 K at high density. The rapid increase in temperature of the electron plasma causes the TBR to have a characteristic time dependence. At short times (less than 100–300 ns), the number of recombined atoms increases rapidly and linearly with time. But as the number of recombined atoms increases and the electron-Rydberg collisions drive the atoms to deeper binding, the temperature of the electron plasma rapidly increases which shuts off further TBR. This leads to a plateau in the number of recombined atoms and, thus, a plateau in the rate of photons from the weakly bound atoms. Because the electron-Rydberg collisions continue, there is steady increase in the rate of photons emitted from the deeply bound states. In the simulations, the fluorescence from the 30 and 57 K plasmas is mainly from the weakly bound atoms, but the fluorescence from the 5 K plasma is a roughly equal combination of deeply bound and weakly bound atoms.

It may be possible that at these lowest temperatures we are entering a regime in which the TBR rate is changing because of the onset of correlations. In Ref. [12] they showed a factor of 2 reduction in the TBR rate when the electron Γ is in the range predicted by this experiment. Predictions of fluorescence from a direct simulation using many-body dynamics would serve as a useful comparison.

Future work could explore recombination fluorescence measurements at even earlier times. Details of the radiative cascade should be explored. In weakly coupled plasmas without perturbed Rydberg series the fluorescence signal should scale as n_0^4. Strongly coupled plasmas have different density scaling due to the rapid temperature dependence at early times. However, at very early times there may be evidence for deviations of TBR from the standard treatment.

In conclusion, we have demonstrated a new fluorescence technique to study three-body recombination in ultracold neutral plasmas at times less than 1 μs that probes the evolution of deeply bound Rydberg states. In calcium, the signal is influenced by strong perturbers in the Rydberg series that make the fluorescence signal proportional to the recombined Rydberg density. At high initial electron temperatures the recombination rate scales as n_0^3 in agreement with theory. However, at low initial electron temperatures the recombination rate scales as $n_0^{2.2}$. When disorder-induced heating and electron-Rydberg scattering are considered for the electron system, our simulation produces a weaker density scaling that is in rough agreement with the experiments. However, the simulation results are only qualitative for the lowest initial electron temperatures.

This work is supported in part by the Research Corporation, the National Science Foundation (Grant No. PHY-0601699), and the Chemical Sciences, Geosciences, and Biosciences Division of the Office of Basic Energy Sciences, U.S. Department of Energy.

[1] T. C. Killian, S. Kulin, S. D. Bergeson, L. A. Orozco, C. Orzel, and S. L. Rolston, Phys. Rev. Lett. **83**, 4776 (1999).
[2] C. E. Simien, Y. C. Chen, P. Gupta, S. Laha, Y. N. Martinez, P. G. Mickelson, S. B. Nagel, and T. C. Killian, Phys. Rev. Lett. **92**, 143001 (2004).
[3] E. A. Cummings, J. E. Daily, D. S. Durfee, and S. D. Bergeson, Phys. Rev. Lett. **95**, 235001 (2005).
[4] T. C. Killian, Science **316**, 705 (2007).
[5] M. S. Murillo, Phys. Rev. Lett. **96**, 165001 (2006).
[6] T. Pohl, T. Pattard, and J. M. Rost, Phys. Rev. Lett. **94**, 205003 (2005).
[7] T. Pohl and T. Pattard, J. Phys. A **39**, 4571 (2006).
[8] T. C. Killian, M. J. Lim, S. Kulin, R. Dumke, S. D. Bergeson, and S. L. Rolston, Phys. Rev. Lett. **86**, 3759 (2001).
[9] J. L. Roberts, C. D. Fertig, M. J. Lim, and S. L. Rolston, Phys. Rev. Lett. **92**, 253003 (2004).
[10] S. Kulin, T. C. Killian, S. D. Bergeson, and S. L. Rolston, Phys. Rev. Lett. **85**, 318 (2000).
[11] S. D. Bergeson and R. L. Spencer, Phys. Rev. E **67**, 026414 (2003).
[12] S. G. Kuzmin and T. M. O'Neil, Phys. Plasmas **9**, 3743 (2002).
[13] F. Robicheaux and J. D. Hanson, Phys. Rev. Lett. **88**, 055002 (2002).
[14] F. Robicheaux and J. D. Hanson, Phys. Plasmas **10**, 2217 (2003).
[15] S. G. Kuzmin and T. M. O'Neil, Phys. Rev. Lett. **88**, 065003 (2002).
[16] R. S. Fletcher, X. L. Zhang, and S. L. Rolston, Phys. Rev. Lett. **99**, 145001 (2007).
[17] S. Mazevet, L. A. Collins, and J. D. Kress, Phys. Rev. Lett. **88**, 055001 (2002).
[18] P. Gupta, S. Laha, C. E. Simien, H. Gao, J. Castro, T. C. Killian, and T. Pohl, Phys. Rev. Lett. **99**, 075005 (2007).
[19] S. Laha, P. Gupta, C. E. Simien, H. Gao, J. Castro, T. Pohl, and T. C. Killian, Phys. Rev. Lett. **99**, 155001 (2007).
[20] P. Mansbach and J. Keck, Phys. Rev. **181**, 275 (1969).
[21] Y. Hahn, Phys. Lett. A **264**, 465 (2000).
[22] T_c also depends on screening and finite temperature effects. See Ref. [5] and references therein.
[23] F. Robicheaux, Phys. Rev. A **70**, 022510 (2004).
[24] M. Miyabe, C. Geppert, M. Kato, M. Oba, I. Wakaida, K. Watanabe, and K. D. A. Wendt, J. Phys. Soc. Jpn. **75**, 034302 (2006).
[25] J. A. Armstrong, P. Esherick, and J. J. Wynne, Phys. Rev. A **15**, 180 (1977).
[26] M. Pajek and R. Schuch, Hyperfine Interact. **108**, 185 (1997).
[27] M. Pajek and R. Schuch, Phys. Scr. **T80**, 307 (1999).